Anal Bioanal Chem
DOI 10.1007/s00216-015-8491-y

RESEARCH PAPER

Monitoring RAYT activity by surface plasmon resonance biosensor

Markéta Bocková · Tomáš Špringer · Iva Nečasová · Jaroslav Nunvar · Bohdan Schneider · Jiří Homola

Received: 14 November 2014 / Revised: 22 December 2014 / Accepted: 13 January 2015

Abstract The process of DNA transposition involves the binding, cleavage, and recombination of specific DNA segments (transposable elements, TE) and is catalyzed by special enzymes encoded by the TE transposases. REP-associated tyrosine transposases (RAYTs) are a class of Y1 nucleases related to the IS_{200}/IS_{605} transposases associated with a bacterial TE known as repetitive extragenic palindrome elements (REPs). Although RAYT has been subject of numerous studies, where DNA binding and cleavage by RAYT have been confirmed for *Escherichia coli*, the molecular mechanism of DNA insertion has not been fully understood. In this work, it is demonstrated that surface plasmon resonance (SPR) biosensor technology combined with a system of DNA hairpin probes (mimicking the natural REP sequence) and short oligonucleotides (ONs) can provide a rapid and real-time platform for monitoring and quantification of RAYT activity. We utilized RAYT from *E. coli* (strain MG1655) as a model system, where we evaluated its activity towards both a natural REP sequence as well as REP sequences having modifications targeting specific features of the DNA crucial for the DNA binding and cleavage. The characteristics of the RAYT-DNA interaction obtained by means of the SPR approach were compared with the results of SDS-PAGE analysis.

Keywords Surface plasmon resonance · REP-associated tyrosine transposase · Biosensor

Published in the topical collection *Direct Optical Detection* with guest editors Guenter Gauglitz and Jiří Homola.

M. Bocková · T. Špringer · J. Homola (✉)
Institute of Photonics and Electronics AS CR, v. v. i., Chaberská 57, 182 51 Prague, Czech Republic
e-mail: homola@ufe.cz

I. Nečasová · J. Nunvar · B. Schneider
Institute of Biotechnology AS CR, v. v. i., Vídeňská 1083, 142 20 Prague, Czech Republic

Introduction

Transposable elements (TEs) are a vast, diverse group of mobile genetic elements present in most genomes. TEs have been extensively studied, especially in bacteria, where they play an important role in genome remodeling and horizontal gene transfer; furthermore, they have shown the ability to sequester and transmit a variety of genes involved in host cell functions, such as antibiotic resistance, catabolism of unusual compounds, virulence factors, pathogenicity, or symbiosis [1–3]. Transposition requires cleavage at the TE ends and their transfer from one genomic location to another. TEs encode an enzyme, the transposase, which catalyzes these reactions: Transposases are able to bind, cleave, and rejoin (or recombine) specific segments of DNA. A variety of transposases with structural and mechanistic diversions have evolved to carry out transposition via several different pathways [4].

Repetitive extragenic palindrome elements (REPs) are one of the best characterized groups of prokaryotic TEs and represent a distinct class of abundant repeats important in the regulation of certain bacterial functions [5]. These REPs form nucleotide stem-loop structures and are often clustered into groups of structures referred to as bacterial interspersed mosaic elements (BIMEs), resembling the sub-terminal hairpins of simple bacterial TEs that encode Y1 transposase. Y1 transposase recognizes and binds hairpins formed by imperfect palindromes (IP) located very close to the ends of the TE.

Recently, Nunvar et al. described the association between REPs and putative Y1 transposase of the IS_{200}/IS_{605} family referred to as REP-associated tyrosine transposases (RAYTs) or $TnpA_{REP}$ [6]. To better understand the functional relationship between REP and its associated RAYT, sequence analyses of selected bacterial representatives were compared to other members of IS_{200}/IS_{605} family. As suggested by these sequence analyses, RAYT shares general organizational and catalytic characteristics with the IS_{200}/IS_{605} family [7]. Sequence

Published online: 31 January 2015

analyses of REP elements suggest that they may form a single-stranded stem-loop; such an architecture has indeed been observed in a crystal structure of the RAYT/REP complex from *Escherichia coli* [8].

These observed interactions suggest that the binding of DNA is mediated primarily through the sugar-phosphate backbone of the DNA hairpin secondary structure and the tetranucleotide guide sequence positioned 5′ to the hairpin foot. The site-specific cleavage of the bound DNA strand is mediated by an active-site tyrosine residue, and results in the formation of a covalent 5′ phosphotyrosine linked intermediate on one side of the ssDNA break and a free 3′ –OH group on the other [9, 10]. However, unlike other IS_{200}/IS_{605} transposases, RAYT is a monomer and is active only in the presence of manganese [8]. Although the DNA binding and the cleavage by RAYT have been previously confirmed, the molecular mechanism of DNA insertion remains unknown. Understanding this mechanism, therefore, remains an important research goal and is expected to provide insight into genome organization and the evolution of bacteria and, furthermore, could possibly help answer the question how REPs have expanded to populate their host genomes.

The DNA binding and cleavage activity of RAYT have been demonstrated in vitro (typically by monitoring of the co-migration of DNA and RAYT) using size exclusion chromatography, separation on SDS-PAGE gel, and electrophoretic mobility shift assay (EMSA) [11, 12]. Although these methods provide sufficient sensitivity, they are rather laborious and typically require labeling or additional means of visualization of interacting biomolecules. Moreover, they only provide semi-quantitative information on the DNA/RAYT interaction. There remains great potential for the use of label-free biosensors to provide quantitative information for these interactions. The use of label-free biosensors based on surface plasmon resonance (SPR) has previously been successfully applied to study several DNA-protein interactions. These studies include the quantification of interactions related to DNA processing in cell [13, 14], as well as studies examining the rates of prolongation or cleavage of DNA immobilized on a SPR sensor surface [15, 16].

In this work, we demonstrate the ability of SPR biosensor technology to monitor and quantify RAYT activity using a specific system of biotinylated DNA hairpin probes and short oligonucleotides (ONs). After incubation with RAYT, these short ONs will hybridize to specific segments of the biotinylated DNA hairpin probes immobilized on the SPR biosensor surface, making it possible to distinguish the cleaved/non-cleaved portions of the probes. Specifically, we investigate RAYT from *E. coli* (strain MG1655) and evaluate its ability to cleave DNA by means of both a natural REP sequence and REP sequence with modifications targeting specific features of the DNA crucial for the DNA binding and cleavage. The influence of Mn^{2+} on the RAYT activity is also studied. Finally, the interaction of RAYT and REP (both natural and modified) are independently examined by SDS-PAGE, and the results are compared with the data obtained using the SPR biosensor.

Materials and methods

Chemical reagents

N-Hydroxysuccinimide (NHS) and 1-ethyl-3-(3-dimethylaminopropyl) carbodiimide hydrochloride (EDC) were obtained from GE Healthcare, USA. Carboxy-terminated [HS–$(CH_2)_{11}$–EG_6–OCH_2–COOH] and hydroxy-terminated [HS–$(CH_2)_{11}$–EG_4–OH] alkanethiols were purchased from Prochimia, Poland. Ethanolamine (EA) and streptavidin from *Streptomyces avidinii* were purchased from Sigma-Aldrich, USA. Ethanol for spectroscopy (purity 99.9 % or greater) was purchased from Merck, USA. All other chemical reagents were purchased in molecular biology grade or higher. Buffers SA_{10} (10 mM sodium acetate, pH 5), PBS (1.4 mM KH_2PO_4, 8 mM Na_2HPO_4, 2.7 mM KCl, 137 mM NaCl, pH 7.4), PBS_{NaCl} (1.4 mM KH_2PO_4, 8 mM Na_2HPO_4, 2.7 mM KCl, 750 mM NaCl, pH 7.4), $Tris_{Mg}$ (50 mM Tris, 50 mM NaCl, 5 mM $MgCl_2$, pH 7.4), $Tris_{Mg,Mn}$ ($Tris_{Mg}$ buffer with 5 mM $MnCl_2$, pH 7.4), heparin elution buffer (20 mM NaH_2PO_4, 2 M NaCl, 1 mM TCEP, pH 7.4), Ni^{2+} binding buffer (20 mM NaH_2PO_4, 500 mM NaCl, 1 mM TCEP, pH 7.4), Ni^{2+} elution buffer (Ni^{2+} binding buffer with 500 mM imidazole), heparin binding buffer (20 mM NaH_2PO_4, 500 mM NaCl, 1 mM TCEP, pH 7.0), and DNA cleavage buffer (50 mM Tris, 50 mM NaCl, 5 mM $MnCl_2$, 1 mM EDTA, 0.5 mM TCEP, pH 7.5) were prepared using deionized water (18 MΩ/cm resistivity, Direct-Q from Millipore).

Oligonucleotides

Biotinylated 76- or 60-mer DNA oligonucleotides (probes) and short 18- or 15-mer DNA oligonucleotides complementary to specific segments of biotinylated probes were purchased from Integrated DNA Technologies (USA) at HPLC-purified grade. Sequences of the oligonucleotides are shown in Table 1. The sequence of b-EC corresponds to the natural sequence found in the genome of bacterium *E. coli*. The only exception is the trinucleotide (TTT) at the 5′ end, which was added for the stabilization of the duplex formed between probe and complementary oligonucleotide C-5 or $C\text{-}5_{TAGA}$. Secondary structures of the biotinylated probes and the complementarity of short oligonucleotides to the specific segments of probes are shown in Fig. 1.

Table 1 Sequence of oligonucleotides used in this study

	Name	Sequence
Target probe	b-EC	5'- TTT CG ATT TTG TAG GAC GGA TAA GGC GTT TAC GCC GCA TCC GGC AGT TGT ACG CAG GTG CCT GAT GCG ACG CTG GC-3'-TEG-biotin
Reference probes	b-EC(TAGA)	5'- TTT CG ATT TTT AGA GAC GGA TAA GGC GTT TAC GCC GCA TCC GGC AGT TGT ACG CAG GTG CCT GAT GCG ACG CTG GC-3'-TEG-biotin
	b-EC(GA)	5'- TTT CG ATT TTG TAG GAC GGA TAA GGC GTT TAC GCC GCA TCC GGC AGT TGT ACG CAG GTG CGA GAT GCG ACG CTG GC-3'-TEG-biotin
	b-EC(no GTAG)	5- C GGA TAA GGC GTT TAC GCC GCA TCC GGC AGT TGT ACG CAG GTG CCT GAT GCG ACG CTG GC-3'-TEG-biotin
	b-EC(duplex)	5'- TTT CG ATT TTG TAG GAC GGA TGC GGC GTT TAC GCC GCA TCC GGC AGT TGT ACG CAG GTG CCT GAT GCG ACG CTG GC-3'-TEG-biotin
	b-EC(random)	5'- TTT CG ATT TTG TAG GAC CAA GAA CAG ATT TAT CTG GCC TTG GGC AGT TGT ACG CAG GTG CCT GAT GCG ACG CTG GC-3'-TEG-biotin
Short complementary oligonucleotides	C-5	5'- TCC TAC AAA ATC GAA ATA -3'
	$C\text{-}5_{TAGA}$	5'- TCT CTA AAA ATC GAA ATA -3'
	C-middle	5'- GCA CCT GCG TAC AAC TGC -3'
	C-3	5'- GCC AGC GTC GCA TCA -3'

Blue lettering denotes tetranucleotide guide sequence, bold lettering denotes nucleotides in hairpin stem, and red lettering the changes in the natural sequence of b-EC. Underlined CT dinucleotide denotes the preferred cleavage site

RAYT expression and purification

The gene of *E. coli* RAYT or $tnpA_{rep}$ (strain MG1655) with a C-terminal His-tag was a kind gift of Dr. Chandler, Laboratoire de Microbiologie et Génétique Moléculaires Centre National de la Recherche Scientifique, Toulouse, France. The wild-type RAYT protein was expressed according to Messing et al. [8], with minor modifications. The His-tag encoding sequence was removed by inserting a stop codon after serine 165 by site-directed mutagenesis in pBS176 vector. A new vector called pBAD-RAYT-WT was transformed to Top10 cells. The initial inoculant was grown in LB broth with addition of 0.5 % glucose overnight and then transferred into 2 L of LB broth at a dilution of approximately 1:60 and grown at 42 °C to an optical density (OD) 0.4 (measured as absorbance at a wavelength of 600 nm). After this optical density was achieved, the culture was cooled down to 18 °C. At OD 0.6, expression was induced by the addition of 0.04 % arabinose. After 18 h, the cells were centrifuged and resuspended in heparin binding buffer. The following steps were performed at 4 °C. Cells were lysed by ultrasound, and the cytosolic fraction was separated by centrifugation at 40,000*g* for 30 min using a Beckman Coulter Avanti J-30I. This fraction was loaded onto a HisTrap Heparin HP column (GE Healthcare) pre-equilibrated in heparin binding buffer. Elution was done by a linear gradient with heparin elution buffer. Eluted fractions containing RAYT protein were loaded onto a HisTrap HP column (GE Healthcare) pre-equilibrated in Ni^{2+} binding buffer and eluted using a linear gradient with Ni^{2+} elution buffer. Purified fractions of RAYT protein were dialyzed three times in DNA cleavage buffer, each dialysis took 2 h. After dialysis, RAYT was concentrated to a final concentration of approximately 20 μM.

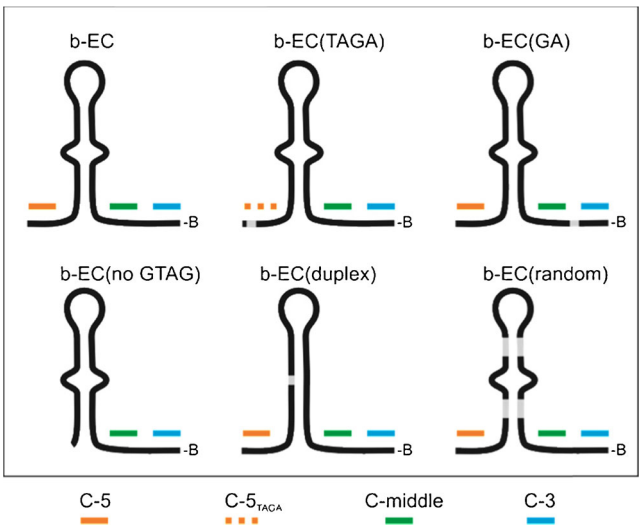

Fig. 1 Schematic representation of the secondary structures of biotinylated DNA probes and complementarity of short oligonucleotides to specific segments of each DNA probe. *Gray sections* denote changes in the natural sequence of b-EC

SPR biosensor

In this study, we used a laboratory four-channel SPR platform based on the wavelength spectroscopy of surface plasmons (Plasmon IV) [17] combined with dispersionless microfluidics [18], both developed at the Institute of Photonics and Electronics, Czech Republic. In this SPR biosensor, the sensor response is expressed as a shift in the wavelength of SPR resonance and is directly proportional to the mass of biomolecules attached to the surface of the sensor. Using the calibration procedure described in Ref. [19], the surface density of both the immobilized probes and the subsequently attached molecules can be determined. For an SPR resonance of around 750 nm, the shift of 1 nm in the SPR wavelength represents a change in the protein surface coverage of 17 ng/cm^2 [19]. All the experiments were performed at 37 °C and under a flow rate of 20 μl/min. Immobilization of biotinylated probes onto the surface of the SPR biosensor chips was achieved via streptavidin covalently attached to a ω-carboxyalkylthiol self-assembled monolayer (SAM). The preparation of mixed SAMs of HS–C_{11}–$(EG)_4$–OH and HS–C_{11}–$(EG)_6$–OCH_2–COOH alkylthiols and in situ immobilization of streptavidin is described in detail in Ref. [20]. In order to provide reproducible binding conditions, the same amount of streptavidin (1.7×10^{12}

streptavidin/cm^2, corresponding to a SPR sensor response of 10 nm) was immobilized on a surface of SPR chip prior to each detection experiment. After the immobilization of streptavidin, $Tris_{Mg}$ was flowed along the sensing surface. Then, 25 nM of biotinylated DNA hairpin probes dissolved in $Tris_{Mg}$ was flowed until the desired surface probe coverage was achieved. Finally, probe-coated surface was incubated with $Tris_{Mg}$. The SPR assay (see below) was optimized in terms of DNA surface coverage to achieve the maximum sensitivity and specificity. Four different values of surface coverage of b-EC were tested: 0.43, 0.85, 1.15, and 1.49 probes/cm^2, which corresponded to 26, 53, 71, and 92 % of the maximum probe coverage respectively. Stability of the biosensor was characterized in terms of stability of the baseline. The baseline stability was determined from ten experiments (using data from two channels on five different chips) to be better than 0.009 nm per 10 min.

RAYT activity assay

We designed a system of biotinylated DNA hairpin probes and short oligonucleotides (ONs) to monitor the cleavage of target DNA by RAYT transposase. The principle of the SPR-based experiment is illustrated in Fig. 2. Two separate channels (detection and reference) were identically functionalized with the same DNA hairpin probe. The detection channel was then incubated with RAYT (so that the DNA cleavage could occur), while the reference channel was incubated only with running buffer. We then quantified the amount of cleaved probes in both detection and reference channels by using three consecutive hybridization/regeneration cycles of short ONs complementary to three separate segments of the immobilized DNA probes. The RAYT activity assay was optimized in terms of RAYT incubation time to achieve the maximum amount of cleaved DNA hairpin probes. Incubation times ranging from 15 to 35 min were tested. As no major effect of the incubation time on the experimental results was observed (data not shown), the incubation time of 20 min was used in our experiments.

The SPR assay was comprised of the following steps. A solution of 500 nM RAYT in $Tris_{Mg,Mn}$ was injected for 20 min in the detection channel (and $Tris_{Mg}$ without RAYT in reference channel), followed with a 10-min injection of $Tris_{Mg}$. Then, washing steps involving a sequence of PBS_{NaCl} (3 min), $Tris_{Mg}$ (7 min), 5 mM NaOH (5 min), and $Tris_{Mg}$ were applied in both detection and reference channels to remove non-specifically adsorbed molecules. To quantify the amount of the remaining DNA on the surface, solutions of 100 nM C-5 (or C-5_{TAGA}), 200 nM C-3, or 200 nM C-middle were flowed for 10 min followed with $Tris_{Mg}$ for 10 min in both the detection and reference channels (performed in a subsequent manner). Prior to the injection of ON, any previous complementary ON was removed by a 2-min injection of 5 mM NaOH to regenerate the sensor surface. In the case of experiments in the absence of Mn^{2+}, 500 mM RAYT in $Tris_{Mg}$ was injected in the detection channel. All the experiments were carried out within 36 h following the preparation of RAYT. The study of enzyme aging was performed over a period of 9 days after the preparation of RAYT.

Depending on whether the DNA cleavage occurred or not, the equilibrium sensor response to the hybridization of a complementary short ON in the reference channel (SR_{ref}) will differ from the equilibrium sensor response of a complementary short ON in the detection channel (SR_{det}). If cleavage did not occur, SR_{det} and SR_{ref} will be identical (applied for all of the three short ONs). If the cleavage of DNA probes took place, SR_{det} and SR_{ref} values depart from each other, and their difference depends on the specific short ON in use. For C-5 and C-middle (ONs complementary to the 5′ end and middle part of DNA probe, respectively), SR_{det} is significantly lower than SR_{ref} because the 5′ end and middle part of DNA hairpin probes were cleaved off. For C-3, SR_{det} is higher than SR_{ref} because the total negative charge on the sensor surface is lower and the 3′ ends of the cleaved DNA probes become more easily accessible for the C-3 complement than 3′ ends (which remained a part of DNA hairpin probes). It should be noted that, in Fig. 2, the SPR signal in the detection channel represents sensor response in the ideal case, where 100 % of the DNA hairpin probes were cleaved off. A typical sensorgram corresponding to the consecutive hybridization of C-3, C-5, and C-middle short ON respectively to the b-EC probe is shown in Fig. 3.

Analysis of RAYT cleavage activity by SDS-PAGE

DNA hairpin probes were dissolved in PBS buffer and heated to a temperature of 95 °C for 15 min and then quickly cooled in ice bath to form a stem-loop structure. These respective DNA hairpin probes were then mixed with RAYT in a 1:1 molar ratio. These reaction mixtures were incubated at 37 °C for 45 min, after which the reaction was stopped by the addition of EDTA at a final concentration of 5 mM. The products were analyzed by SDS-PAGE in which DNA was visualized by a silver stain and the protein by a Coomassie stain. SDS-PAGE analysis was performed three times: immediately after the preparation of RAYT, 3 days, and 7 days after the preparation of RAYT.

Results and discussion

In the assay proposed in Fig. 2, two separate channels were identically functionalized with the same DNA hairpin probe. RAYT (which cleaved the specific DNA sequence) was injected into the detection channel while only a running buffer was injected into the reference channel. A short washing step

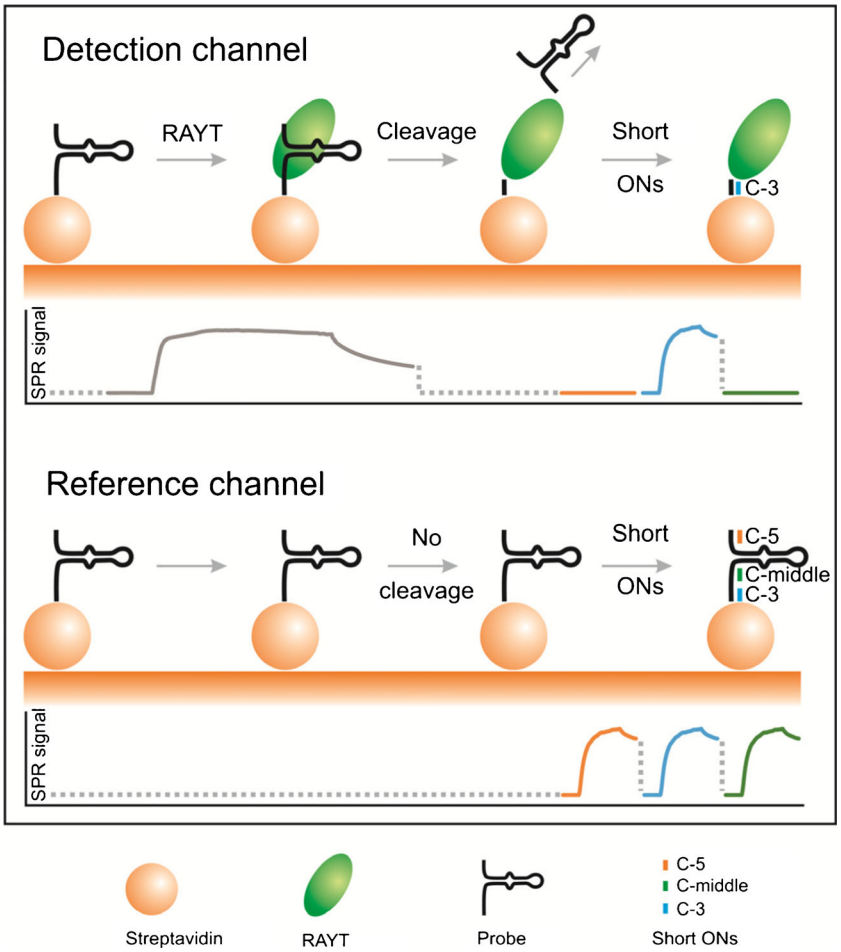

Fig. 2 Schematic principle of the SPR assay

was included in both channels to remove non-specifically adsorbed molecules, which was followed by three consecutive hybridization/regeneration cycles of each short ONs to monitor the cleaved/non-cleaved segments of the DNA hairpin probe. A regeneration procedure was developed to allow for the removal of the bound short ONs from the sensor surface ensuring repeated use of the SPR chip. We did not observe any significant loss of activity after the regeneration step or any cross-reactivity among respective ONs (data not shown). The concentration of complementary ONs was set, such that the sensor surface reached an equilibrium state within 10 min.

It should be noted that the sensor response to the RAYT binding was several times higher (up to 6 nm) than expected (for a 1:1 RAYT:DNA probe interaction, the maximum specific sensor response should be around 2.2 nm) due to the non-specific adsorption of positively charged RAYT to the sensor

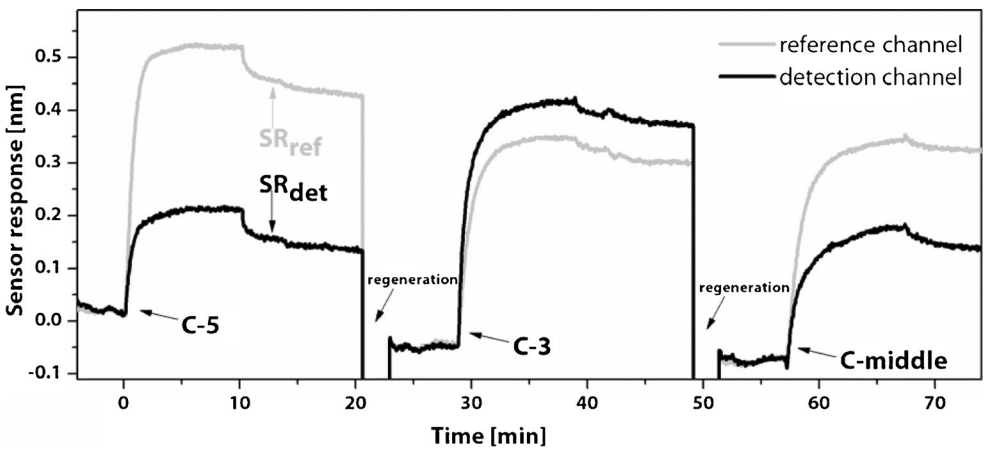

Fig. 3 Temporal sensor response to the consecutive hybridization/regeneration of C-3, C-5 and C-middle short ONs, respectively

surface with negatively charged DNA probes. While this non-specific adsorption prevents direct monitoring of the RAYT activity and DNA probe cleavage, it has only minor effect on the proposed assay.

Optimization of the assay

We studied the influence of the surface probe density (PD) on RAYT cleavage efficiency (CE) in experiments where b-EC and C-5 complementary short ONs were used as a model system. A dispersionless microfluidic system was used to obtain a desired PD, which allows for precise control over the amount of sample delivered to the SPR surface.

CE is defined as the relative amount of immobilized DNA hairpin probes that were cleaved by RAYT and was calculated as $CE=(SR_{ref}-SR_{det})/SR_{ref}$, where SR_{ref} and SR_{det} denote the equilibrium sensor response to the complementary short ON in the reference and detection channel, respectively. The efficiency of ON hybridization (HE) is defined as the ratio of the formed duplexes to immobilized DNA hairpin probes and was calculated as $HE=SR_{ON}\times M_{probe}/(SR_{probe}\times M_{ON})$, where M_{probe} and M_{ON} are the molecular weights of the DNA hairpin probe and short ON, respectively, SR_{probe} is the equilibrium sensor response to the immobilization of the DNA hairpin probe, and SR_{ON} is the sensor response to the hybridization of short ON.

We tested four different PDs of b-EC target hairpin probes. Table 2 shows the sensor response to the binding of C-5 complementary ON in the detection (SR_{det}) and reference channel (SR_{ref}) along with calculations of CE and HE.

As anticipated, the sensor response to the C-5 binding (both SR_{ref} and SR_{det}) increased with the amount of immobilized b-EC probes; however, the sensor response in the detection channel (SR_{det}) for low PDs was very low and, therefore, exhibited a higher level of noise. While the HE did not change significantly with the PD (decreases only from 75 to 71 %), the CE decreased substantially (from 85 to 52 %). This can be explained by both the presence of steric crowding of the immobilized probes and by the electrostatic repulsion of their negatively charged sugar-phosphate backbones [21, 22]. Moreover, it is possible that RAYT molecules bound to DNA probes could spatially hinder the access of other RAYT molecules and thus reduce CE. Due to the near-palindromic sequence of the hairpin stem and the length of the hairpin probes (76-mer), a wide distribution of inter-strand duplexes and intra-strand hairpin structures formed on the surface of the SPR biosensor may be expected. We suggest that, at lower PD values, the equilibrium is shifted towards the hairpin structure that contributes to ability of RAYT to cleave DNA. In the following experiments reported herein, a surface PD of 1.15×10^{12} probes/cm^2 was used, which provides both a high RAYT cleavage efficiency and a sufficiently high sensor response in the detection channel.

Table 2 Surface probe density (PD) of the immobilized b-EC hairpin probes and corresponding sensor response to the binding of C-5 complementary ON in the detection channel (SR_{det}) and reference channel (SR_{ref}) and calculated hybridization efficiency (HE) and cleavage efficiency (CE) values

PD [10^{12} probes/cm^2]	C-5		HE [%]	CE [%]
	SR_{det} [nm]	SR_{ref} [nm]		
0.43	0.027	0.171	75	85
0.85	0.086	0.353	78	76
1.15	0.153	0.451	74	66
1.49	0.271	0.56	71	52

Measurement of RAYT activity

The RAYT from *E. coli* (strain MG1655) interacts with the target REP through a recognition mode that exploits both the DNA hairpin secondary structure and the 5′ GTAG guide tetranucleotide. In addition, it has been suggested that the cleavage process is CT dinucleotide specific, generating a RAYT/REP covalent adduct, and may only take place in the presence of manganese [8]. To demonstrate the specificity and sensitivity of the SPR-based assay, we measured the RAYT activity with the natural REP sequence (b-EC) as well as several modifications to the REP sequence (or interaction conditions). These modifications targeted features crucial for the RAYT/REP interaction and consisted of a mutation in the GTAG tetranucleotide or its complete deletion, aberrations in secondary hairpin structure or the cleavage site, and the absence of Mn^{2+}.

The quantification of the amount of cleaved hairpin probes can be accomplished through comparison of SR_{det} and SR_{ref} (equilibrium sensor response to the hybridization of complementary short ON in detection and reference channel, respectively). A detailed description of relationship between SR_{det} and SR_{ref} for each short ON was given above (see "Materials and methods"). The SR_{det}/SR_{ref} ratios for respective DNA hairpin probes are presented in Fig. 4. These values were determined from at least three independent experiments. It is clear that for Fig. 4a (C-5) and Fig. 4b (C-middle), a lower ratio indicates a higher amount of cleaved hairpin probes (or lower amount of cleaved probes in the case of C-3 short ON). This suggests that C-5 short ON is the most sensitive indicator of the RAYT cleavage activity and that SR_{det}/SR_{ref} ratio for C-5 is the most suitable parameter for the evaluation of the RAYT cleavage activity in the presented study. The chip-to-chip reproducibility of the SPR biosensor response to the binding of short ONs in the reference channel was better than 93 %, regardless of the DNA hairpin probe used. The reproducibility values were determined from at least four independent experiments for each DNA hairpin probe.

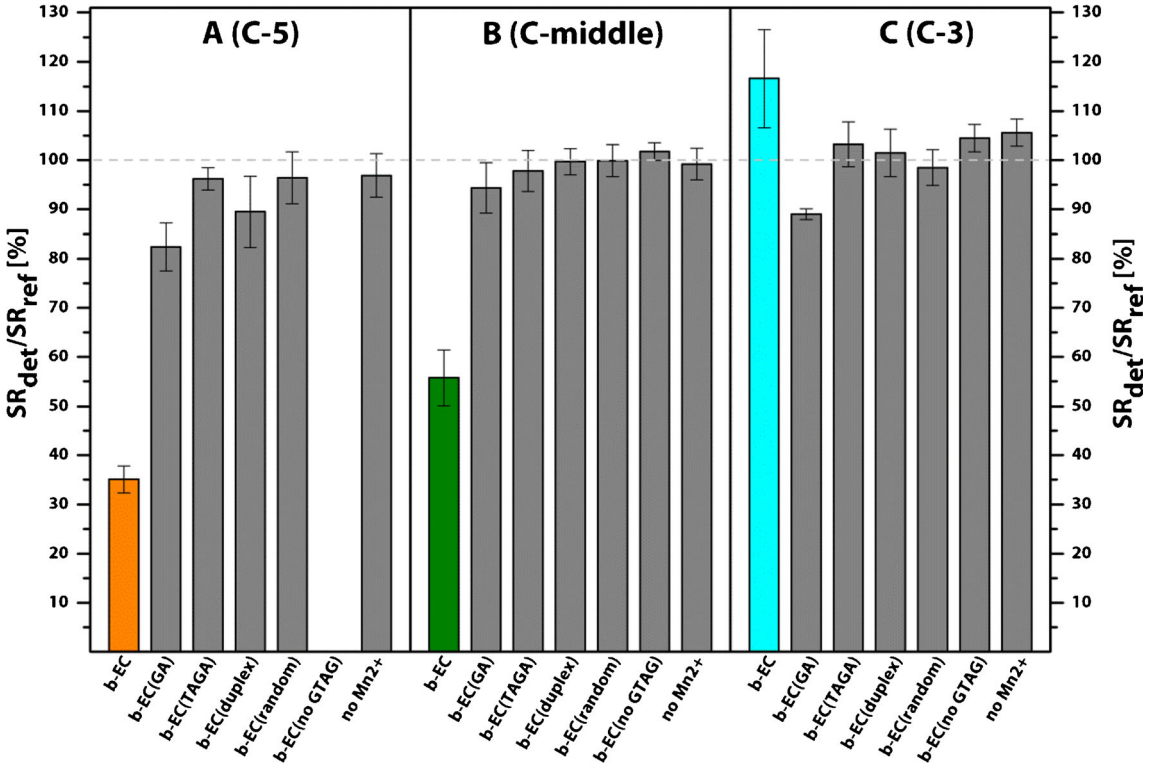

Fig. 4 The ratios (mean ± standard deviation) of SR_{det} and SR_{ref} for respective DNA hairpin probes and C-5 (**A**), C-3 (**B**), and C-middle (**C**) complementary short ONs

The data in Fig. 4 show a decrease in SR_{det}/SR_{ref} ratio for the C-5 and C-middle (orange and green bars in Fig. 4a, b, respectively) and an increase in SR_{det}/SR_{ref} ratio for C-3 (cyan bar in Fig. 4c), suggesting that RAYT binds and cleaves the b-EC target DNA hairpin probe that mimics the natural REP sequence. The RAYT cleavage activity was also confirmed by SDS-PAGE analysis, as shown in Fig. 5 line 4, where the covalent complex between RAYT and the 3′-end oligonucleotide of the cleaved DNA migrates in polyacrylamide gel more slowly than RAYT alone due to its larger molecular weight. The bend corresponding to the RAYT-DNA covalent complex is seen between 20 and 25 kDa.

Apart from to the natural REP-mimicking probe, a substantial decrease in the SR_{det}/SR_{ref} ratio at C-5 was also observed for the b-EC(GA)-modified DNA probe. Although the sequence of b-EC(GA) had a mutation (see Table 1) in the CT

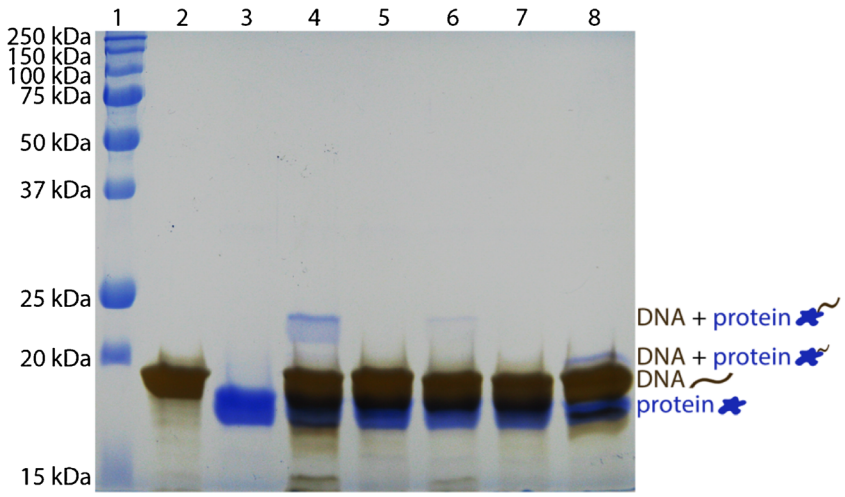

Fig. 5 SDS-PAGE (denaturating conditions) analysis of RAYT cleavage. DNA was visualized by a silver stain and protein by a Coomassie stain. *Lines* are defined as follows: *1* marker of molecular weight, *2* b-EC alone, *3* RAYT protein alone, *4* RAYT + b-EC, *5* RAYT + b-EC(TAGA), *6* RAYT + b-EC(duplex), *7* RAYT + b-EC(random), *8* RAYT + b-EC(GA). *Labels on the right* point to bands proving the DNA cleavage by RAYT. *Higher bands in lines 4*, *6*, and *8* indicate the covalent adduct between RAYT and cleaved fragment of respective DNA

dinucleotide cleavage site situated closer to the hairpin [$(CT)_h$], RAYT was still able to cleave the b-EC(GA) probe at another CT dinucleotide positioned downstream the natural sequence [$(CT)_d$]. The cleavage occurs with a lower yield with respect to the natural b-EC probe, generating a shorter 3′-end DNA fragment. This finding is also supported by the results of the SDS-PAGE analysis (Fig. 5, line 8) and agrees well with the suggestion that there is a considerable flexibility in the location of CT dinucleotide sequence relative to the DNA hairpin [7]. The comparison of the SR_{det}/SR_{ref} ratio at C-5 for b-EC (35 %) and b-EC(GA) (82 %) indicates that $(CT)_h$ presents a preferred cleavage site to $(CT)_d$: If the cleavage sites were equal, the SR_{det}/SR_{ref} ratio for b-EC(GA) would be around 60 %. The partial cleavage at $(CT)_d$ is supported by a decrease in the SR_{det}/SR_{ref} ratio at C-3 for b-EC(GA) as well. This is believed to be caused by a very low stability of the duplex formed by C-3 and the 3′ end of the cleaved b-EC(GA) probe, where only four nucleotides are available for hybridization in contrast to 15 nucleotides in the case of cleavage at $(CT)_h$ position. However, the cleavage activity at $(CT)_d$ could be limited by steric effects, as $(CT)_d$ is located closer to the sensor surface.

It is worth noting that when the SPR-based assay was performed with b-EC(duplex) modified probe, in which the naturally occurring base mismatches in the hairpin stem were mutated to form canonical Watson-Crick base pairs, a cleavage was observed, yet with lower efficiency (evidenced by decrease in the SR_{det}/SR_{ref} ratio at C-5). This finding was also in agreement with the results of the SDS-PAGE analysis (Fig. 5, line 6). The band representing the RAYT-b-EC(duplex) covalent adduct was weaker than in the case of unmodified b-EC, which could indicate that the mismatches in the stem are not necessary for the cleavage, as proposed by Messing et al. [8].

All other mutations in the natural REP sequence disrupted RAYT cleavage activity, including randomizing the nucleotides in the hairpin while maintaining the hairpin structure [b-EC(random)], the absence of GTAG [b-EC(no GTAG)], or its mutation [b-EC(TAGA)] (Figs. 4 and 5). The absence of Mn^{2+} ions also prevented the cleavage. These results are consistent with the findings of Messing et al. [8].

In order to demonstrate that the proposed method provides a rapid and convenient platform for quantitative analysis of RAYT activity, we performed a series of experiments with the target hairpin probe b-EC and short ONs, where the RAYT cleavage efficiency was determined, as described above, as a function of the time after preparation. As follows from the temporal dependence in Fig. 6 (left), CE decreases in time from 66 to 2 % for C-5 and from 42 to 2 % for C-middle, respectively. This decrease implies a higher amount of non-cleaved DNA hairpin probes on the surface of the biosensor. In case of C-3 short ON, CE gains negative values (SR_{det} is higher than SR_{ref}). The diminishing ability of RAYT to cleave DNA brings a higher total negative charge on the surface and less accessible 3′ ends of non-cleaved DNA probes. Therefore, CE for C-3 increases in time from −21 to −2 %. Gradual decrease in activity of RAYT is confirmed by the results of SDS-PAGE analysis (Fig. 6, right). The higher band in lane 4 becomes weaker over time, suggesting that RAYT activity was indeed decreasing.

The amounts of RAYT (4 μg) and DNA oligonucleotides (100 ng) necessary for the SPR biosensor-based assay are considerably lower than the amounts needed for SDS-PAGE (approximately 8 μg of RAYT and 9 μg of DNA oligonucleotides

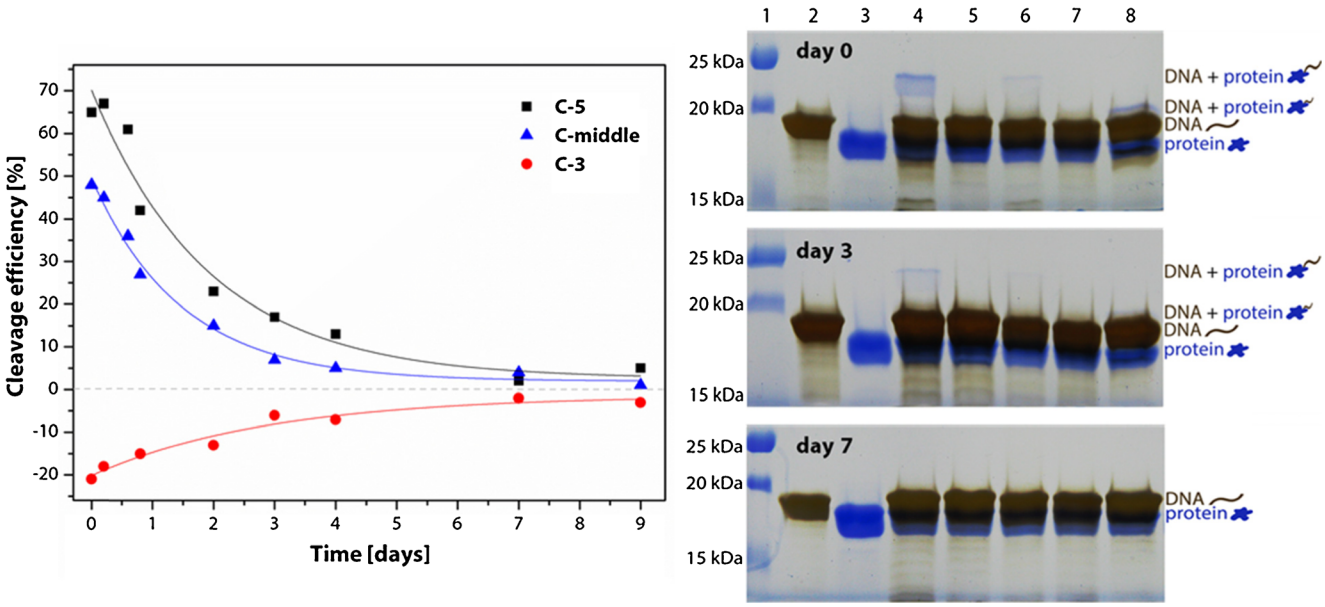

Fig. 6 Dependence of RAYT cleavage activity on time using the SPR biosensor (*left*). Results of SDS-PAGE analysis (*right*). For description of lines of the gels, see caption for Fig. 5

for one reaction). Moreover, the amount of short oligonucleotides used in SPR biosensor is several orders of magnitude higher than the limit of detection for short oligonucleotides achieved by SPR biosensors.

Conclusions

We demonstrated that SPR biosensors can be used to characterize the enzymatic activity of transposases. Specifically, we investigated the ability of RAYT from *E. coli* (strain MG1655) to cleave DNA using a natural REP sequence and sequences with modifications targeting specific features in the DNA crucial for the DNA binding and cleavage. The characteristics of the RAYT-DNA interaction obtained using the SPR biosensor technology were compared with those obtained by SDS-PAGE analysis. The results suggest that (1) the imperfect palindrome in DNA hairpin stem is not necessary for the interaction, and (2) even though the cleavage occurs with the highest efficiency at the CT dinucleotide in the preferred location, it can also occur at a more distant CT site, albeit with a lower efficiency. The presented approach is expandable to other types of systems and presents a rapid and quantitative platform for study of interaction characteristics of transposases as well as their activity.

Acknowledgments This research was supported by Praemium Academiae of the Academy of Sciences of the Czech Republic, the Czech Science Foundation under contract # GAP305/12/1801, by BIOCEV CZ.1.05/1.1.00/02.0109 from the ERDF and by RVO 86652036 and RVO 67985882.

References

1. Delihas N (2008) Small mobile sequences in bacteria display diverse structure/function motifs. Mol Microbiol 67:475–481
2. Boccard F, Prentki P (1993) Specific interaction of IHF with RIBs, a class of bacterial repetitive DNA elements located at the 3′ end of transcription units. EMBO J 12:5019–5027
3. Higgins CF, McLaren RS, Newbury SF (1988) Repetitive extragenic palindromic sequences, mRNA stability and gene expression: evolution by gene conversion? A review. Gene 72:3–14
4. Curcio MJ, Derbyshire KM (2003) The outs and ins of transposition: from mu to kangaroo. Nat Rev Mol Cell Biol 4:865–877
5. Horvath P, Barrangou R (2010) CRISPR/Cas, the immune system of bacteria and archaea. Science 327:167–170
6. Nunvar J, Huckova T, Licha I (2010) Identification and characterization of repetitive extragenic palindromes (REP)-associated tyrosine transposases: implications for REP evolution and dynamics in bacterial genomes. BMC Genomics 11
7. Ton-Hoang B, Siguier P, Quentin Y, Onillon S, Marty B, Fichant G, Chandler M (2012) Structuring the bacterial genome: Y1-transposases associated with REP-BIME sequences. Nucleic Acids Res 40:3596–3609
8. Messing SAJ, Ton-Hoang B, Hickman AB, McCubbin AJ, Peaslee GF, Ghirlando R, Chandler M, Dyda F (2012) The processing of repetitive extragenic palindromes: the structure of a repetitive extragenic palindrome bound to its associated nuclease. Nucleic Acids Res 40:9964–9979
9. Barabas O, Ronning DR, Guynet C, Hickman AB, Ton-Hoang B, Chandler M, Dyda F (2008) Mechanism of IS200/IS605 family DNA transposases: activation and transposon-directed target site selection. Cell 132:208–220
10. Hickman AB, James JA, Barabas O, Pasternak C, Ton-Hoang B, Chandler M, Sommer S, Dyda F (2010) DNA recognition and the precleavage state during single-stranded DNA transposition in D. radiodurans. EMBO J 29:3840–3852
11. Lee HH, Yoon JY, Kim HS, Kang JY, Kim KH, Kim DJ, Ha JY, Mikami B, Yoon HJ, Suh SW (2006) Crystal structure of a metal ion-bound IS200 transposase. J Biol Chem 281:4261–4266
12. Ronning DR, Guynet C, Ton-Hoang B, Perez ZN, Ghirlando R, Chandler M, Dyda F (2005) Active site sharing and subterminal hairpin recognition in a new class of DNA transposases. Mol Cell 20:143–154
13. Hegde V, Wang M, Deutsch WA (2004) Human ribosomal protein S3 interacts with DNA base excision repair proteins hAPE/Ref-1 and hOGG1. Biochem Us 43:14211–14217
14. Ioannou C, Schaeffer PM, Dixon NE, Soultanas P (2006) Helicase binding to DnaI exposes a cryptic DNA-binding site during helicase loading in Bacillus subtilis. Nucleic Acids Res 34:5247–5258
15. Šípová H, Vaisocherová H, Štěpánek J, Homola J (2010) A dual surface plasmon resonance assay for the determination of ribonuclease H activity. Biosens Bioelectron 26:1605–1611
16. Vaisocherová H, Snášel J, Špringer T, Šípová H, Rosenberg I, Štěpánek J, Homola J (2009) Surface plasmon resonance study on HIV-1 integrase strand transfer activity. Anal Bioanal Chem 393: 1165–1172
17. Pimková K, Bocková M, Hegnerová K, Suttnar J, Čermák J, Homola J, Dyr JE (2012) Surface plasmon resonance biosensor for the detection of VEGFR-1-a protein marker of myelodysplastic syndromes. Anal Bioanal Chem 402:381–387
18. Špringer T, Piliarik M, Homola J (2010) Surface plasmon resonance sensor with dispersionless microfluidics for direct detection of nucleic acids at the low femtomole level. Sensors Actuators B Chem 145:588–591
19. Homola J (2006) Surface plasmon resonance based sensors. Wolfbeis OS (ed). Vol. 4 Germany, Berlin: Springer
20. Vaisocherová H, Zítová A, Lachmanová M, Štěpánek J, Králíková S, Liboska R, Rejman D, Rosenberg I, Homola J (2006) Investigating oligonucleotide hybridization at subnanomolar level by surface plasmon resonance biosensor method. Biopolymers 82:394–398
21. Špringer T, Šípová H, Vaisocherová H, Štěpánek J, Homola J (2010) Shielding effect of monovalent and divalent cations on solid-phase DNA hybridization: surface plasmon resonance biosensor study. Nucleic Acids Res 38:7343–7351
22. Xu F, Pellino AM, Knoll W (2008) Electrostatic repulsion and steric hindrance effects of surface probe density on deoxyribonucleic acid (DNA)/peptide nucleic acid (PNA) hybridization. Thin Solid Films 516:8634–8639